JACS
JOURNAL OF THE AMERICAN CHEMICAL SOCIETY
Article
pubs.acs.org/JACS

Microfluidic Study of Fast Gas–Liquid Reactions

Wei Li,[†] Kun Liu,[†] Ryan Simms,[†] Jesse Greener,[†] Dinesh Jagadeesan,[†] Sascha Pinto,[‡] Axel Günther,[‡] and Eugenia Kumacheva*,[†]

[†]Department of Chemistry, University of Toronto, Toronto, Ontario M5S 3H6, Canada

[‡]Department of Mechanical & Industrial Engineering, University of Toronto, 5 King's College Road, Toronto, Ontario M5S 3G8, Canada

Supporting Information

ABSTRACT: We present a new concept for studies of the kinetics of fast gas–liquid reactions. The strategy relies on the microfluidic generation of highly monodisperse gas bubbles in the liquid reaction medium and subsequent analysis of time-dependent changes in bubble dimensions. Using reactions of CO_2 with secondary amines as an exemplary system, we demonstrate that the method enables rapid determination of reaction rate constant and conversion, and comparison of various binding agents. The proposed approach addresses two challenges in studies of gas–liquid reactions: a mass-transfer limitation and a poorly defined gas–liquid interface. The proposed strategy offers new possibilities in studies of the fundamental aspects of rapid multiphase reactions, and can be combined with throughput optimization of reaction conditions.

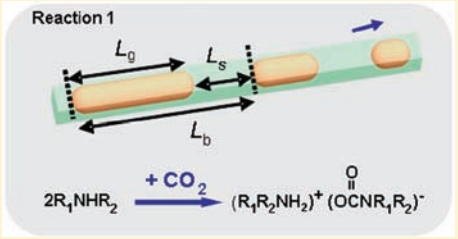

INTRODUCTION

Gas–liquid reactions such as the sequestration of CO_2 by aqueous alkanolamines, the reaction of H_2S with aqueous ferric sulfate, or the hydrogenation, fluorination, and chlorination of organic molecules are of great practical importance.[1,2] To generate new, efficient catalysts and optimized chemical formulations, fundamental knowledge has to be developed on the mechanisms of gas–liquid reactions and their kinetic and thermodynamic characteristics. Currently, rate constants of rapid gas–liquid reactions determined by conventional methods have large (up to ±35%) variations,[3,4] for at least two reasons. First, the reaction rate is limited by the rate of gas transfer through the gas–liquid interface. In order to overcome this mass-transfer limitation, gas–liquid reactions are studied in reactors with mechanically agitated stirring; however, the kinetic data obtained by this method are sensitive to the relative position of the stirrer.[5,6] Second, a poorly defined interface between the gas and liquid phases leads to uncertainty in determining the mass-transfer parameters. This problem is partly solved by using wetted-wall columns, in which liquid reaction medium is evenly distributed as a thin film at the gas–liquid interface;[7,8] however, the mass-transfer limitation still persists.[3]

Recently, microfluidics (MFs) has opened new, exciting opportunities in fundamental studies of chemical reactions such as glycosylation, synthesis of carbamates, oxidation, and reduction.[9−12] In particular, multiphase MF reactors offer advantages of large and well-defined interfacial areas, fast mixing, and reduced mass-transfer limitations.[13] In comparison with conventional batch reactions, multiphase reactions conducted in a MF format allow precise control of reaction conditions, high product yield and conversion, and enhanced selectivity.[14] Microfluidic studies of reactions occurring in liquid–liquid reaction systems, that is, in droplets suspended in a continuous liquid phase, enable kinetic studies of reactions on the millisecond time scale by monitoring the change in intensity of a fluorescent dye compartmentalized in the droplets.[15,16] Yet, MF studies of the kinetics of fast gas–liquid reactions (which may take a fraction of a second) remain a challenge.[17−19] For example, a study of hydrogenation of cyclohexene in a multiphase packed-bed reactor yielded mass-transfer coefficients that were nearly 2 orders of magnitude larger than the values obtained in standard laboratory-scale reactors, and the gas–liquid interface was not well-defined.[20] A study of CO_2 absorption by an aqueous NaOH solution in a falling film microreactor exhibited a mass-transfer limitation, as well as flow maldistribution.[21] In addition, conventional Fourier transform infrared (FT-IR) spectroscopy is not suitable for fast gas–liquid reactions: the reaction time is shorter than the acquisition time of even a single FT-IR scan,[22] whereas a series of data points are required to investigate reaction kinetics.[23]

Here we propose a new strategy for studies of the kinetics of rapid gas–liquid reactions that overcomes the two main drawbacks described above. The method includes the MF generation of bubbles of a reactive gas in the liquid reaction medium and subsequent analysis of the reaction-controlled change in the dimensions of the bubbles as they move through the downstream microchannel. In addition to the determination of rate constants, the MF method can be used for comparative studies of the efficiency of various gas-binding agents and for the throughput screening of reaction conditions.

Received: October 31, 2011
Published: December 15, 2011

   dx.doi.org/10.1021/ja2101278 | J. Am. Chem.Soc. 2012, 134, 3127−3132

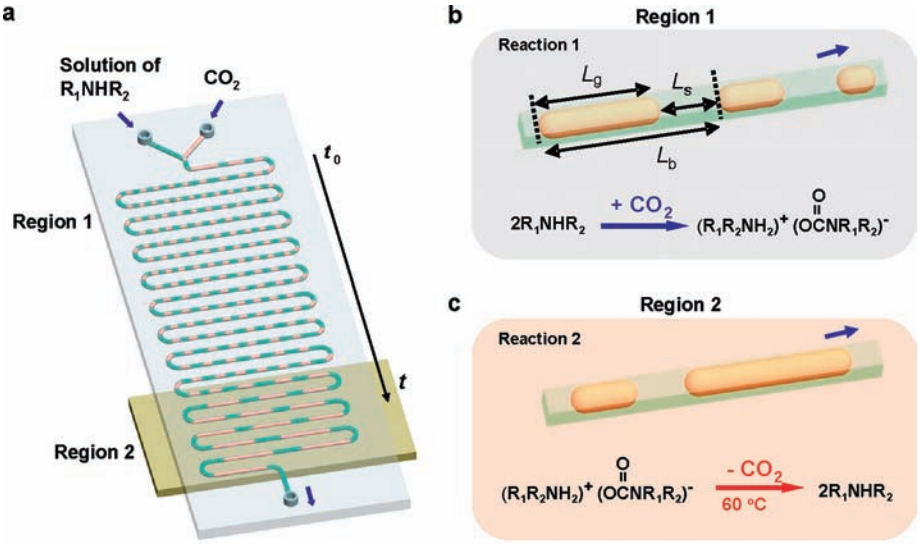

Figure 1. Reversible CO_2 binding to secondary amines conducted in the MF reactor. (a) Schematic of the MF reactor. Reactions 1 and 2 (shown in (b) and (c)) occur in regions 1 and 2, respectively. An ITO glass-based heater (shown as a light-brown plate) is introduced underneath region 2. An aluminum plate (not shown in the schematic) is placed underneath region 1, in order to maintain the temperature in region 1 at 23 °C. The blue arrows show the direction of flow of the fluids in the MF reactor. The height and the width of the microchannel are 125 and 150 μm, respectively; the length of the microchannel is 605 mm. (b) Reaction of CO_2 with a secondary amine yields a carbamate salt (reaction 1). The volume of CO_2 plugs (orange color) decreases as CO_2 reacts with R_1NHR_2. (c) Release of CO_2 mediated by the increase in temperature (reaction 2) leads to the expansion of CO_2 plugs.

The proposed MF method offers the following useful characteristics: (i) small dimensions of the microchannels (on the order of 10^{-6}m), which provide a short distance for gas mass transfer in a liquid phase;[24,25] (ii) generation of highly monodisperse gas bubble (plugs) separated by liquid slugs comprising a binding agent, which leads to a well-defined gas–liquid interfacial area;[26−28] (iii) good mixing in the liquid slugs and absence of cross-contaminations between adjacent slugs;[13] and (iv) a correlation between the distance traveled by the reagents and the reaction time through a so-called "distance-to-time transformation",[15] as well as rapid data acquisition.

As an exemplary reaction, we used the reversible binding of CO_2 to secondary amines discovered by Jessop et al.[29] The reaction of CO_2 with a low-polarity liquid transforms the latter into an ionic liquid, whereas subsequent heating of the system or purging it with an inert gas releases CO_2 and recovers the low-polarity liquid. The solvent "polarity switch" offers a promising green chemistry application by eliminating the need to replace solvents in multistep reactions, as well as other important applications;[30−32] however, progress in applications of this group of reactions is undermined by the lack of fundamental understanding of the reaction kinetics.[33]

We also verified the applicability of the proposed MF method to the reaction of CO_2 with *N*-methyldiethanolamine dissolved in water. The value of the rate constant determined using our MF method was within the range determined by using a stirring-cell reactor and a wetted-column reactor.

■ RESULTS AND DISCUSSION

Figure 1 shows a schematic of the MF reactor used in the present work, the experimental design, and the chemical reactions between CO_2 and an exemplary binding agent. Gaseous CO_2 and the solution of R_1NHR_2 in acetonitrile are supplied to the two inlets of the MF reactor (Figure 1a). At the Y-junction of the reactor, the gaseous stream breaks up in a periodic manner and generates CO_2 plugs that are separated with a liquid-filled space (slugs). The reaction between CO_2 and R_1NHR_2 (reaction 1 in Figure 1) starts at the Y-junction, where the reagents come in contact, and continues in region 1 of the MF reactor, yielding a carbamate salt. The reverse reaction (reaction 2) is triggered by heating region 2 of the reactor.

Figure 1b,c shows the direct and reverse reactions between CO_2 and R_1NHR_2, respectively, and the notations for the lengths of gaseous plugs and liquid slugs. When CO_2 plugs travel through region 1, their volume is reduced (Figure 1b) due to the mass transfer of CO_2 from the gas phase into the liquid, which is accompanied by reaction 1. (We note that the drop in pressure along the microchannel favors plug expansion; however, this effect is slower and weaker than that caused by the mass transfer and reaction 1, which dominate over short distances from the Y-junction.) Thus, the stabilized volume of the CO_2 plugs corresponds to the equilibrium of the direct and reverse reactions.

We note that, at room temperature, the equilibrium is strongly shifted toward reaction 1.[34,35] In the present work, the concentration of R_1NHR_2 in acetonitrile did not exceed 10 wt %, in order to avoid a significant change in the properties of the solution (Table S1) and the formation of the precipitate in the solution of the carbamate salt in acetonitrile, as well as the temperature of the system due to exothermic reaction 1. Subsequent to reaction 1, heating of region 2 favors the reverse reaction (reaction 2), which yields R_1NHR_2 and CO_2, thereby leading to an increase in the volume of the plugs (Figure 1c).

We studied the kinetics of reaction 1 by monitoring the reduction in the length of CO_2 plugs with reaction time. The original dimensions of the plugs were sufficiently large to preserve their plug-like shape upon completion of reaction 1, which allowed us to assume that the gaseous plugs and the liquid slugs move with the same velocity[36] and, in this manner, to convert the distance that they traveled into the reaction time. We measured the average velocity of the CO_2 plugs in the

dx.doi.org/10.1021/ja2101278 | *J. Am. Chem.Soc.* 2012, 134, 3127−3132

different regions of the microchannel (separated by various distances from the Y-junction) and determined the reaction time as the ratio of a particular distance over the locally averaged velocity of the CO_2 plugs (see Supporting Information). We defined a "unit cell" length (L_b) as the sum of the lengths of the CO_2 plug (L_g) and the adjacent liquid slug (L_s) (Figure 1b). The volume, V_g , of the CO_2 plugs was calculated as $V_g = A(L_g - d_h) + (\pi d_h^3/6)$, where A and d_h are the cross-section area and the hydraulic diameter of the CO_2 plug, respectively. The volume of the liquid adjacent to the CO_2 plugs in the "unit cell' was calculated as $V_s = L_b A' - V_g$, where A' is the area of the cross-section of the microchannel (Figure S1).

We used a solution of *N*-ethylbutylamine (NHEtBu) in acetonitrile as a binding agent. The CO_2 plugs generated in the solution of NHEtBu underwent a dramatic shrinkage as they traveled in the downstream channel (Figure 2a). At a distance

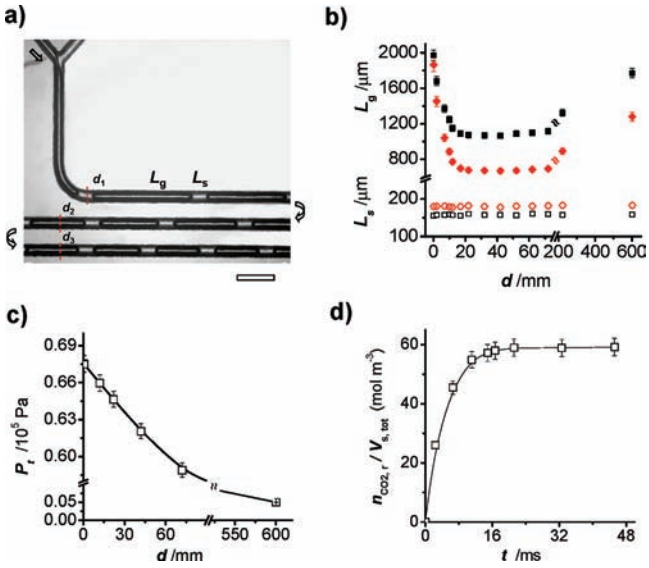

Figure 2. Characterization of reaction 1. (a) Optical microscopy image of the CO_2 plugs (dark color), which are separated by the liquid slugs (light color) of the 4.0 wt % solution of NHEtBu in acetonitrile. The arrows show the direction of fluid flow in the microchannel. The vertical red dashed lines show representative positions at which the measurements of plug length took place, that is, d_1, d_2, and d_3, corresponding to the distances of 2, 12, and 22 mm, respectively, from the Y-junction. The scale bar is 500 μm. (b) Variation in the mean length of CO_2 plugs, L_g (black solid squares, red solid diamonds), and the length of liquid slugs, L_s (black open squares, red open diamonds), in acetonitrile (squares) and in the 4.0 wt % solution of NHEtBu in acetonitrile (diamonds), plotted as a function of the distance, d, from the Y-junction. (c) Estimated variation in pressure in the MF reactor (Table S1). (d) Variation in the number of moles of CO_2 reacted with NHEtBu, normalized by the volume, $V_{s,tot}$, of the neighboring liquid slug in a "unit cell", plotted as a function of time t. The flow rate of the 4.0 wt % solution of NHEtBu in acetonitrile was 3.2 mL h^{-1}. The inlet pressure of CO_2 was 0.68×10^5 Pa (with respect to standard pressure of 1.01×10^5 Pa).

of ~22−72 mm from the Y-junction, the length of the plugs was almost invariant. These two trends are shown in Figure 2b, where the variations in the mean lengths of the gaseous plugs and liquid slugs (L_g and L_s, respectively) are plotted as a function of the distance from the Y-junction. We also conducted a control experiment, that is, the generation and dissolution of the CO_2 plugs in acetonitrile. In the system under study and in the control systems, the lengths of the liquid slugs remained constant over the course of experiments; however, the stabilized mean length of the CO_2 plugs was ~37% smaller in the solution of NHEtBu in acetonitrile than in the control experiment (Figure 2b). In both systems, the length of the gaseous plugs began to increase when the distance from the Y-junction exceeded ~70 mm, due to the dominant effect of the decrease in pressure in the plugs as they moved toward the outlet (the pressure at the outlet was 1.01×10^5 Pa).

The rate of reaction 1 was characterized by the change in the ratio $n_{CO_2,r}/V_{s,tot}$ with reaction time t, where $n_{CO_2,r}$ is the number of moles of reacted CO_2 and $V_{s,tot}$ is the volume of the slug of the solution of NHEtBu in acetonitrile in a "unit cell" (Figure 1b). The reaction time was determined as $t = d/U_b$, where d is the distance from the Y-junction and U_b is the velocity of the CO_2 plugs (see Table S1). The ratio $n_{CO_2,r}/V_{s,tot}$ was calculated as

$$n_{CO_2,r}/V_{s,tot} = n_{CO_2,tot}/V_{s,tot} - n_{CO_2,d}/V_{s,d} \quad (1)$$

where $n_{CO_2,tot}$ and $n_{CO_2,d}$ are the numbers of moles of CO_2 sequestered at time t by the solution of NHEtBu in acetonitrile and by pure acetonitrile, respectively, and $V_{s,d}$ is the slug volume in pure acetonitrile. We assumed that CO_2 behaves as an ideal gas and that the effect of the temperature change upon CO_2 dissolution is insignificant.[37] The number of moles of CO_2 sequestered by the solution of NHEtBu in acetonitrile was then determined as

$$n_{CO_2,tot} = (P_0V_0 - P_tV_t)/RT \quad (2)$$

where P_0 and P_t are the pressures of CO_2 at the inlet and in the MF reactor at time t, respectively, and V_0 and V_t are the volumes of the CO_2 plugs at $t \approx 0$ (immediately after the Y-junction) and at time t, respectively. Similarly, in the control system the value of $n_{CO_2,d}$ was determined as

$$n_{CO_2,d} = (P_0V_0' - P_t'V_t')/RT \quad (3)$$

where P_t' is the pressure of CO_2 at time t, and V_0' and V_t' are the volumes of CO_2 plugs at $t \approx 0$ and at time t, respectively.

The initial pressure of CO_2 was set to $P_0 = 0.68 \times 10^5$ Pa (all the pressures in the present work are reported relative to standard pressure of 1.01×10^5 Pa). In the course of the reaction, the pressure P_t changed owing to reaction 1, the dissolution of CO_2 in acetonitrile, and the change in hydrodynamic resistance along the microchannel.[38] The variation in pressure in the reactor (Figure 2c) was estimated by calculating the friction factor and the streamwise pressure gradient in the channel (see Table S1).[39] Figure 2d shows the variation in the ratio $n_{CO_2,r}/V_{s,tot}$ with reaction time. Following a sharp increase in $n_{CO_2,r}/V_{s,tot}$ within the first 15 ms of the reaction, the system reached equilibrium, at which point 58 ± 3 mol m^{-3} of CO_2 reacted with NHEtBu.

To determine the rate constant of reaction 1, we studied the temporal variation in the ratio $n_{CO_2,r}/V_{s,tot}$ at various concentrations of NHEtBu in acetonitrile (NHEtBu was the rate-limiting reagent). Figure 3a shows that in the NHEtBu concentration range from 4.0 to 10 wt % (corresponding to the molar concentration from 0.31 to 0.78 mol L^{-1}), the amount of reacted CO_2 and the rate of its consumption increased at a higher concentration of NHEtBu, suggesting a higher rate of reaction 1 and no mass-transfer limitation. For all the

dx.doi.org/10.1021/ja2101278 | J. Am. Chem.Soc. 2012, 134, 3127−3132

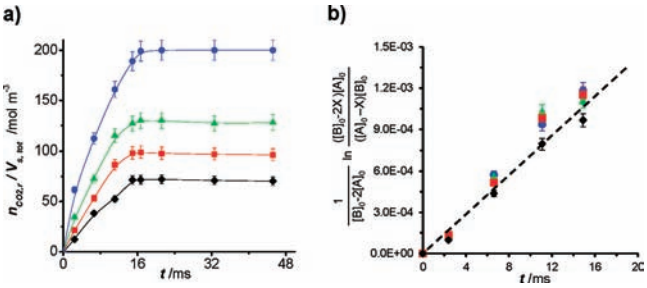

Figure 3. Kinetics of reaction 1. (a) Variation in the normalized number of moles of reacted CO_2, $n_{CO_2,r}/V_{s,tot}$, plotted as a function of reaction time t for solutions of NHEtBu in acetonitrile. The concentrations of NHEtBu are 4.0 (black diamonds), 6.0 (red squares), 8.0 (green triangles), and 10 wt % (blue circles). The lines are given for eye guidance. (b) Variation in kt (see eq 4) plotted as a function reaction time t, where k is the rate constant for reaction 1 at 23 °C. The slope of the trend line yields the value of k. The symbols correspond to the concentrations given in (a). The inlet pressure of CO_2 was 0.59×10^5 Pa. The flow rate of the liquid phase was 3.2 mL h^{-1}.

concentrations of NHEtBu, the ratio $n_{CO_2,r}/V_{s,tot}$ remained invariable after the first ~16 ms, indicating that reaction 1 reached an equilibrium.

Since the rate of the reaction $CO_2 + 2R_1R_2NH \rightarrow R_1R_2NH_2 + R_1R_2NCOO$ is determined by the rate of the first step, that is, the second-order reaction $CO_2 + R_1R_2NH \rightarrow R_1R_2NCOOH$,[2,33] we applied eq 4 to the kinetics of reaction 1 as in ref 40:

$$kt = \frac{1}{[B]_0 - 2[A]_0} \ln \frac{([B]_0 - 2X)[A]_0}{([A]_0 - X)[B]_0} \quad (4)$$

where $[A]_0$ and $[B]_0$ are the initial concentrations of CO_2 and NHEtBu, respectively, in the liquid phase, $X = n_{CO_2,r}/V_{s,tot}$ is the concentration of CO_2 reacted at time t, and k is the reaction rate constant. For reaction 1, $X = X_p$, where X_p is the concentration of the carbamate salt in the liquid phase. We assumed that at a particular moment of time $[A]_0 = n_{CO_2,tot}/V_{s,tot}$. In the range of $[B]_0$ from 4.0 to 10 wt %, the plot of the variation of the right-hand side term in eq 4 vs t yielded a straight line with the slope equal to $k = 75 \pm 5$ m^3 $kmol^{-1}$ s^{-1} (M^{-1} s^{-1}) (Figure 3b).

By applying a similar approach to studies of the kinetics of the reaction of CO_2 with *N*-dipropylamine (NHPrPr), we found $k = 82 \pm 5$ m^3 $kmol^{-1}$ s^{-1} (M^{-1} s^{-1}). The close values of rate constants for the reactions of CO_2 with NHEtBu and NHPrPr suggested that these two reagents have a similar activity of binding to CO_2.

We also tested the MF method for the reaction of CO_2 with *N*-methyldiethanolamine (MDEA) in an aqueous solution. The overall reaction is $CO_2 + MeN(EtOH)_2 + H_2O \rightarrow Me(EtOH)_2NH^+ + HCO_3^-$. In the first step, MDEA instantaneously reacts with H_2O and forms OH^- ions. It is accepted that reaction rate r of CO_2 with MEDA in water is determined by the reaction rate of CO_2 with OH^- ions (r_{CO_2/OH^-}) and the reaction rate of CO_2 with MDEA ($r_{CO_2/MDEA}$) (eq 5a), and that the overall reaction order is 2 (the reaction of CO_2 with water is usually neglected).[41,42] The overall rate constant, k, is thus determined by the rate constant of the reaction of CO_2 with MDEA ($k_{CO_2/MDEA}$) and the rate constant of the reaction of CO_2 with OH^- ions (k_{CO_2/OH^-}), as in eq 5b.[42,43]

$$r = r_{CO_2/MDEA} + r_{CO_2/OH^-} \quad (5a)$$

$$k = r/[CO_2] = k_{CO_2/MDEA}[MDEA] + k_{CO_2/OH^-}[OH^-] \quad (5b)$$

where [MDEA] and $[OH^-]$ are the concentrations of MDEA and OH^- ions, respectively, and k_{CO_2/OH^-} and $k_{CO_2/MDEA}$ are the rate constant of the reactions of CO_2 with OH^- ions and with MDEA, respectively. Based on the earlier works of Ko et al.[42] and Pinsent et al.,[44] we determined the value of k_{CO_2/OH^-} for T = 296 K (23 °C) by using the relation $\log_{10}(k_{CO_2/OH^-}) = 13.635 - 2895/T$.

In the MF experiments, the dissolution of CO_2 in water at pH = 7.0 was used as a control experiment. The pressure and the velocity the CO_2 plugs were determined as described above. We determined the overall reaction rate constants to be $k = 5.8 \pm 0.1$ and 8.6 ± 0.1 m^3 $kmol^{-1}$ s^{-1} (M^{-1} s^{-1}) for 2 and 4 wt % MDEA aqueous solutions, respectively. For these two solutions, we measured pH to find $[OH^-]$, and subsequently, by using eq 5b, determined $k_{CO_2/MDEA}$ to be 6.4 ± 0.8 m^3 $kmol^{-1}$ s^{-1} (M^{-1} s^{-1}) (Figure 4). This value is in the range of 5−10 m^3 $kmol^{-1}$ s^{-1} (M^{-1} s^{-1}) determined for the reaction of CO_2 with MDEA in an aqueous solution, by using fast mixing and wetted-wall column methods.[41,42]

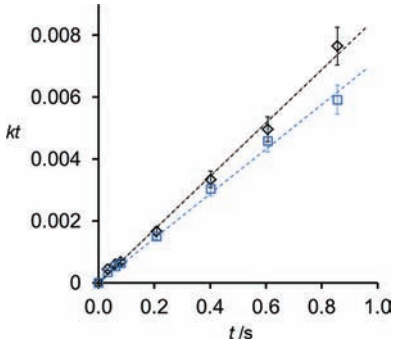

Figure 4. Determination of the rate constant of the reaction of CO_2 with MDEA in an aqueous solution. The variation in $(1/([B]_0 - [A]_0))\ln(([B]_0 - X)[A]_0)/([A]_0 - X)[B]_0)$ (equal to kt) is plotted as a function of the reaction time. The slope of the trend line yields the value of the rate constant k. The concentrations of the aqueous solution of MDEA were 2.0 (blue open squares) and 4.0 wt % (black open diamonds). The flow rate of the liquid phase was 0.8 mL h^{-1}, $P_{CO_2} = 0.97 \times 10^5$ Pa, and the temperature was 23 °C.

In the second series of experiments, subsequent to reaction 1, we triggered the reverse reaction (reaction 2) by increasing the temperature in region 2 from 23 to 60 °C. Upon heating, the CO_2 plugs expanded (Figure 5a). Figure 5b shows the variation in the mean length of the gaseous plugs in the system undergoing reaction 2 and in the control system, both plotted as a function of plug position d in the microchannel. The point of origin corresponds to d = 72 mm, at which the lengths of the CO_2 plugs were stabilized. In both systems, the length of the CO_2 plugs noticeably increased when they entered region 2 (shown in the graph as the shaded gray area); however, the relative increase in the plug length in the solution of NHEtBu

dx.doi.org/10.1021/ja2101278 | J. Am. Chem.Soc. 2012, 134, 3127−3132

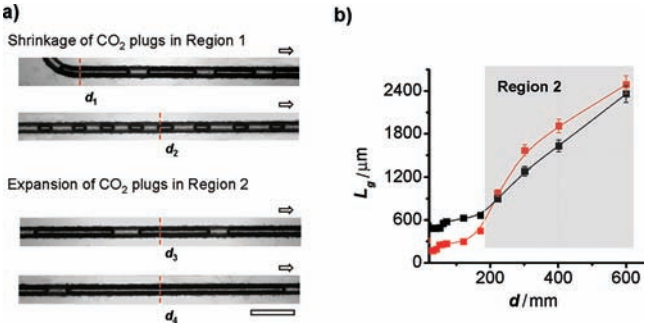

Figure 5. Characterization of reaction 2. (a) Optical microscopy images of CO_2 plugs in 4.0 wt % solution of NHEtBu in acetonitrile at positions d_1–d_4 from the Y-junction: d_1 = 2, d_2 = 42, d_3 = 202, and d_4 = 602 mm. (b) Variation in the mean length of the CO_2 plugs, L_g, in the "unit cell" plotted as a function of distance d for reaction 2 (red squares) and for the dissolution of CO_2 in acetonitrile (black squares). From (a) to (b), the flow rate of 4.0 wt % NHEtBu solution was 3.2 mL h^{-1}; the inlet pressure of CO_2 was 0.57 × 10^5 Pa. The arrows indicate the direction of flow in the microchannel. The scale bar is 500 μm.

in acetonitrile was significantly larger than in the control system. A stronger expansion of the CO_2 plugs in the presence of NHEtBu occurred due to the dissociation of the carbamate salt (reaction 2), in addition to the release of CO_2 from acetonitrile and expansion of CO_2 plugs at 60 °C. We assumed a similar extent of possible minor vaporization of acetonitrile from the control system and from the acetonitrile solution of NHEtBu, and ignored the change in vapor pressure of NHEtBu in the acetonitrile solution.

Using eqs 1–3, we determined the equilibrium concentration of the carbamate salt in acetonitrile after reaction 1 to be X_p = 65 ± 3 mol m^{-3}. The total number of moles, $n_{t,tot}$, of CO_2 remaining in the liquid phase after reaction 2 was determined as $n_{t,tot} = n_{in,tot} - n_{out,tot}$, where $n_{in,tot}$ and $n_{out,tot}$ are the numbers of moles of CO_2 in the gaseous plug at the Y-junction and at the outlet of the MF reactor, respectively. Similarly, in the control system, the number of moles of CO_2 dissolved in acetonitrile was determined as $n_{t,d} = n_{in,d} - n_{out,d}$, where $n_{in,d}$ and $n_{out,d}$ are the numbers of moles of CO_2 in the gas phase at the inlet and the outlet of the reactor, respectively. The number of moles of CO_2 remaining in the continuous liquid phase after reaction 2 was determined as $n_{t,r} = n_{t,tot} - n_{t,d}$. The values of $n_{in,tot}$, $n_{out,tot}$, $n_{in,d}$, and $n_{out,d}$ were calculated using eq 2. The concentration of the carbamate salt, $X_p' = n_{t,r}/V_{s,tot}$, in the solution after completion of reaction 2 was determined to be 15 ± 2 mol m^{-3}. Using the equilibrium concentration of the carbamate salt X_p = 65 ± 3 mol m^{-3} (after completion of reaction 1), we calculated the equilibrium conversion in reaction 2 as $(X_p - X_p')/X_p$ and determined it to be 77 ± 3%.

CONCLUSIONS

A MF method offers the ability to conduct time- and labor-efficient studies of rapid gas–liquid reactions. For such reactions, it offers rapid acquisition of the kinetic data. In addition, the method provides the capability of high-throughput screening of reaction conditions and the selection of new efficient reagents. In our work, the MF method was utilized for systems with relatively low concentrations of the reagents and products and, hence, for the low-viscosity media. Further development is needed to utilize the method for the processes used for CO_2 sequestration in the oil industry.

The MF method can be extended to reactions of CO, H_2, or N_2O in organic solvents.[45–48] These reactions have important applications in CO_2 reduction, hydrogen storage, and activation of small molecules. Furthermore, by measuring rate constants as a function of reaction temperature, the reported method provides the ability to determine thermodynamic characteristics of gas–liquid reactions. The MF method can be further used for high-throughput optimization of reaction conditions. A thorough understanding of the underlying mechanisms of the gas–liquid reactions will provide the basis for the discovery of new, efficient reagents and catalysts.

ASSOCIATED CONTENT

Supporting Information

Methods, determination of the area of a cross-section of the microchannel and of CO_2 plugs, image of microfluidic chip, measurements of the velocity of CO_2 plugs in the microchannel, calculation of reaction time, change in the viscosity and surface tension of amine solution before and after reaction, reduction in pressure along the microreactor, and video clips of CO_2 dissolution and reaction. This material is available free of charge via the Internet at http://pubs.acs.org.

AUTHOR INFORMATION

Corresponding Author

ekumache@chem.utoronto.ca

ACKNOWLEDGMENTS

E.K. gratefully acknowledges financial support by Carbon Management Canada (CMC) and by the Canada Research Chair program (NSERC Canada). A.G. acknowledges NSERC Canada (RTI and Discovery programs).

REFERENCES

(1) Rochelle, G. T. *Science* **2009**, *325*, 1652–1654.
(2) Danckwerts, P. V. *Gas-liquid reactions*; McGraw-Hill: New York. 1970.
(3) Vaidya, P. D.; Kenig, E. Y. *Chem. Eng. Commun.* **2007**, *194*, 1543–1565.
(4) Aboudheir, A.; Tontiwachwuthikul, P.; Chakma, A.; Idem, R. *Chem. Eng. Sci.* **2003**, *58*, 5195–5210.
(5) Kucka, L.; Richter, J.; Kenig, E. Y.; Gorak, A. *Sep. Purif. Technol.* **2003**, *31*, 163–175.
(6) Ebrahimi, S.; Kleerebezem, R.; van Loosdrecht, M. C. M.; Heijnen, J. J. *Chem. Eng. Sci.* **2003**, *58*, 417–427.
(7) Yih, S. M.; Shen, K. P. *Ind. Eng. Chem. Res.* **1988**, *27*, 2237–2241.
(8) Sun, W. C.; Yong, C. B.; Li, M. H. *Chem. Eng. Sci.* **2005**, *60*, 503–516.
(9) Ratner, D. M.; Murphy, E. R.; Jhunjhunwala, M.; Snyder, D. A.; Jensen, K. F.; Seeberger, P. H. *Chem. Commun.* **2005**, 578–580.
(10) Sahoo, H. R.; Kralj, J. G.; Jensen, K. F. *Angew. Chem., Int. Ed.* **2007**, *46*, 5704–5708.
(11) Inoue, T.; Schmidt, M. A.; Jensen, K. F. *Ind. Eng. Chem. Res.* **2007**, *46*, 1153–1160.
(12) Wada, Y.; Schmidt, M. A.; Jensen, K. F. *Ind. Eng. Chem. Res.* **2006**, *45*, 8036–8042.
(13) Günther, A.; Jensen, K. F. *Lab Chip* **2006**, *6*, 1487–1503.
(14) Hartman, R. L.; Jensen, K. F. *Lab Chip* **2009**, *9*, 2495–2507.
(15) Song, H.; Ismagilov, R. F. *J. Am. Chem. Soc.* **2003**, *125*, 14613–14619.
(16) Chan, K. L. A.; Gulati, S.; Edel, J. B.; de Mello, A. J.; Kazarian, S. G. *Lab Chip* **2009**, *9*, 2909–2913.
(17) Kashid, M. N.; Kiwi-Minsker, L. *Ind. Eng. Chem. Res.* **2009**, *48*, 6465–6485.

(18) Yoshida, J. I.; Nagaki, A.; Yamada, T. *Chem.—Eur. J.* **2008**, *14*, 7450−7459.
(19) Hessel, V.; Angeli, P.; Gavriilidis, A.; Löwe, H. *Ind. Eng. Chem. Res.* **2005**, *44*, 9750−9769.
(20) Losey, M. W.; Schmidt, M. A.; Jensen, K. F. *Ind. Eng. Chem. Res.* **2001**, *40*, 2555−2562.
(21) Zanfir, M.; Gavriilidis, A.; Wille, C.; Hessel, V. *Ind. Eng. Chem. Res.* **2005**, *44*, 1742−1751.
(22) The maximum acquisition rate with "rapid scan option" for Bruker Veritex 70-1 is 58 scans/s (17 ms/scan), with 16 cm^{-1} spectral resolution (which is extremely low spectral resolution): http://www.brukeroptics.com/vertex700.html.
(23) Greener, J.; Abbasi, B.; Kumacheva, E. *Lab Chip* **2010**, *10*, 1561−1566.
(24) Beebe, D. J.; Mensing, G. A.; Walker, G. M. *Annu. Rev. Biomed. Eng.* **2002**, *4*, 261−286.
(25) Squires, T. M.; Quake, S. R. *Rev. Mod. Phys.* **2005**, *77*, 977−1026.
(26) Garstecki, P.; Fuerstman, M. J.; Stone, H. A.; Whitesides, G. M. *Lab Chip* **2006**, *6*, 437−446.
(27) Park, J. I.; Nie, Z.; Kumachev, A.; Abdelrahman, A.; Binks, B.; Stone, H.; Kumacheva, E. *Angew. Chem., Int. Ed.* **2009**, *48*, 5300−5304.
(28) Park, J. I.; Nie, Z.; Kumachev, A.; Kumacheva, E. *Soft Matter* **2010**, *6*, 630−634.
(29) Jessop, P. G.; Heldebrant, D. J.; Li, X.; Eckert, C. A.; Liotta, C. L. *Nature* **2005**, *436*, 1102−1102.
(30) Phan, L.; Andreatta, J. R.; Horvey, L. K.; Edie, C. F.; Luco, A. L.; Mirchandani, A.; Darensbourg, D. J.; Jessop, P. G. *J. Org. Chem.* **2008**, *73*, 127−132.
(31) Eckert, C. A.; Liotta, C. L.; Bush, D.; Brown, J. S.; Hallett, J. P. *J. Phys. Chem. B* **2004**, *108*, 18108−18118.
(32) Phan, L.; Brown, H.; White, J.; Hodgson, A.; Jessop, P. G. *Green Chem.* **2009**, *11*, 53−59.
(33) Heldebrant, D. J.; Yonker, C. R.; Jessop, P. G.; Phan, L. *Energy Environ. Sci.* **2008**, *1*, 487−493.
(34) Hampe, E. M.; Rudkevich, D. M. *Tetrahedron* **2003**, *59*, 9619−9625.
(35) Masuda, K.; Ito, Y.; Horiguchi, M.; Fujita, H. *Tetrahedron* **2005**, *61*, 213−229.
(36) Serizawa, A.; Feng, Z.; Kawara, Z. *Exp. Therm Fluid Sci.* **2002**, *26*, 703−714.
(37) Danckwerts, P. V.; Kennedy, A. M. *Chem. Eng. Sci.* **1958**, *8*, 201−215.
(38) Fuerstman, M. J.; Lai, A.; Thurlow, M. E.; Shevkoplyas, S. S.; Stone, H. A.; Whitesides, G. M. *Lab Chip* **2007**, *7*, 1479−1489.
(39) Kreutzer, M. T.; Kapteijn, F.; Moulijn, J. A.; Kleijn, C. R.; Heiszwolf, J. J. *AIChE J.* **2005**, *51*, 2428−2440.
(40) Atkins, P.; de Paula, J. *Physical chemistry*, 7th ed.; W. H. Freeman and Co.: New York, 2002.
(41) Blauwhoff, P. M. M.; Versteeg, G. F.; Van Swaaij, W. P. M *Chem. Eng. Sci.* **1984**, *39*, 207−225.
(42) Ko, J.-J.; Li, M.-H. *Chem. Eng. Sci.* **2000**, *55*, 4139−4147.
(43) Camacho, F.; Sánchez, S.; Pacheco, R.; La Rubia, M. D.; Sánchez, A. *Int. J. Chem. Kinet.* **2008**, *3*, 204−214.
(44) Pinsent, B. R. W.; Pearson, L.; Roughton, F. W. J. *Trans. Faraday Soc.* **1956**, *52*, 1512−1520.
(45) Welch, G. C.; Juan, R. R. S.; Masuda, J. D.; Stephan, D. W. *Science* **2006**, *314*, 1124−1126.
(46) Welch, G. C.; Stephan, D. W. *J. Am. Chem. Soc.* **2007**, *129*, 1880−1881.
(47) Mömming, C. M.; Otten, E.; Kehr, G.; Frohlich, R.; Grimme, S.; Stephan, D. W.; Erker, G. *Angew. Chem., Int. Ed.* **2009**, *48*, 6643−6646.
(48) Otten, E.; Neu, R. C.; Stephan, D. W. *J. Am. Chem. Soc.* **2009**, *131*, 9918−9919.